THE USE OF HOPF BIFURCATIONS LOCI FOR SPURIOUS-FREE NONLINEAR MICROWAVE CIRCUIT DESIGN

Vittorio RIZZOLI (1) and Andrea NERI (2)

(1) Dipartimento di Elettronica, Informatica e Sistemistica, University of Bologna, Villa Griffone, 40044 Pontecchio Marconi, Bologna - ITALY
(2) Fondazione Ugo Bordoni, Villa Griffone, 40044 Pontecchio Marconi, Bologna - ITALY

ABSTRACT

Bifurcation theory is coupled with harmonic-balance techniques into a powerful CAD tool for the design of stable nonlinear microwave circuits and subsystems. Automatically generated Hopf bifurcations loci provide detailed information on the role of selected circuit parameters in the generation of spurious tones, and are effectively used in support to ordinary optimization to produce spurious-free circuit topologies.

INTRODUCTION

The design of nonlinear microwave circuits for steady-state stability is an intriguing aspect of the general CAD problem for which no systematic solutions are presently available in commercial software. Two basic kinds of instabilities may be encountered in microwave circuit operation: *synchronous* instability related to the existence of positive real natural frequencies of the steady state, and *asynchronous* instability due to the appearance of pairs of complex conjugate natural frequencies with positive real parts [1]. The former results in a permanent deviation of the circuit electrical regime from the predicted nominal steady state, the latter in the generation of spurious tones. If the nonlinear analysis is carried out by the Newton-iteration based harmonic-balance (HB) technique, the onset of synchronous instability may be traced back to a sign reversal of one real eigenvalue of the Jacobian matrix **M** of the HB errors with respect to the state-variable harmonics [2], [3], and thus of the Jacobian determinant. A specification on synchronous stability can thus be introduced in a conventional circuit optimization under the form of a suitable lower-bound constraint on the magnitude of det[**M**]. This concept was successfully applied to the numerical design of oscillators for electrical performance and synchronous stability in a recent work [4]. When it comes to asynchronous instability, the computational difficulties are much higher. A spurious oscillation starts to build up when a (secondary) Hopf bifurcation [1] is encountered on the solution path of the circuit parametrized by an arbitrary control parameter [5]. Existing algorithms for the automatic detection of such bifurcations are well suited for analysis purposes [6], [7], but are not fast enough to be used inside an optimization loop. Also, it is very difficult to express in the form of a minimization constraint the requirement that no Hopf bifurcations exist on the solution path. Thus the spurious-free design of nonlinear microwave circuits is still an unsolved problem.

An interactive solution to this problem is developed for the first time in the present paper. The concept of Hopf bifurcation of a time-periodic regime is first reviewed making use of a unified HB formulation encompassing both forced and autonomous circuits. It is then shown that in the neighborhood of a Hopf bifurcation, a modified form of the HB equations allows the bifurcation to be approximately but accurately located in a very efficient way, i.e., by performing one Newton loop only. This technique provides the basis of a predictor-corrector scheme that can efficiently generate Hopf bifurcations loci in an arbitrary two-dimensional parameter space. In turn, this enables the designer to locate regions of the space of designable circuit parameters where spurious-free operation is likely to take place. A conventional optimization with the variable ranges constrained to such regions then leads to a spurious-free design. If necessary, the process can be iterated in order to find the best tradeoff between the stability requirement and the electrical specifications. The design of a stable varactor-tuned broadband VCO is discussed for illustrative purposes.

HOPF BIFURCATIONS OF TIME-PERIODIC STEADY STATES

Let us consider a nonlinear circuit (either forced or autonomous) continuously depending on a free parameter u, and operating in a time-periodic steady-state regime with a fundamental angular frequency ω_0 (carrier). In order to establish the conditions for the startup of a spurious oscillation, a perturbation analysis of the periodic steady state is carried out. At frequency ω the linear subnetwork is described by the ordinary frequency-domain equations

$$\mathbf{Y}(\omega)\,\mathbf{V}(\omega) + \mathbf{I}(\omega) + \mathbf{N}(\omega) = \mathbf{0} \tag{1}$$

where $\mathbf{V}(\omega)$, $\mathbf{I}(\omega)$ are vectors of voltage and current harmonics at the ports, and $\mathbf{N}(\omega)$ is an equivalent (Norton) representation of the driving sources (including DC bias). $\mathbf{Y}(\omega)$ is the linear subnetwork admittance matrix. Let us assume that for $u = u_H$ an oscillation of vanishingly small amplitude and fundamental frequency ω_H is superimposed on the steady state. The electrical regime is then quasi-periodic with spectral lines at the steady-state harmonics $k\omega_0$ and at the sidebands $k\omega_0 + \omega_H$ (k integer). If $\Delta\mathbf{V}$, $\Delta\mathbf{I}$ are vectors containing all the normalized sideband harmonics, the perturbation equations of the linear subnetwork can be written

$$\mathbf{Y}_L\,\Delta\mathbf{V} + \Delta\mathbf{I} = \mathbf{0} \tag{2}$$

where $\mathbf{Y}_L$ is a block-diagonal matrix whose diagonal blocks are given by $\mathbf{Y}(\omega)$ computed at the sidebands. Furthermore, in the neighborhood of the steady state the nonlinear subnetwork can be described by the frequency-conversion equations [8]

$$\mathbf{P}^{-1}\,\Delta\mathbf{V} = \mathbf{Q}^{-1}\,\Delta\mathbf{I} \tag{3}$$

where **P**, **Q** are conversion matrices which can be computed by the algorithm discussed in [8]. By combining (2) and (3) we obtain the numerical condition for the existence of a Hopf bifurcation at $u = u_H$:

$$\det\,[\mathbf{Y}_L\,\mathbf{P} + \mathbf{Q}] \triangleq D(u_H, \omega_H) = 0 \tag{4}$$

CH3577-4/95/0000-1089$01.00 © 1995 IEEE

In the case of an autonomous circuit, the carrier frequency ω_0 is one of the unknowns of the harmonic-balance system, as discussed below. However, it has been shown [5] that to first order, the carrier frequency is unaffected by an asynchronous perturbation. Thus the condition (4) is valid both for forced and autonomous circuits, with the same definition of conversion matrices.

Since D is a complex quantity, (4) is a nonlinear system of two real equations in two unknowns, and in principle its solutions can be found by any system-solving technique. However, the circuit state depends on the parameter u, and in turn the conversion matrices are state-dependent [8]. Thus each iteration requires a numerical solution of the HB equations and a new calculation of the conversion matrices. This procedure is inherently slow, and usually implies severe convergence problems. Better results can be obtained by a stepwise technique based on the numerical construction of the periodic solution path, and on a subsequent search based on Nyquist analysis [6]. The full scan of a solution path by this method typically takes a few hundred seconds on an HP 9000/750 workstation. This is still far too slow to be included in a circuit optimization loop as a part of the objective evaluation process.

In order to overcome this difficulty, the following approximate technique for the detection of Hopf bifurcations has been devised. Let us assume that the spurious has built up to some finite amplitude, so that the steady-state regime is quasi-periodic, with lines at all the intermodulation products of two fundamentals ω_0, ω_S, namely, $k\omega_0 + h\omega_S$ (k, h integers). Let **E** be the vector of real and imaginary parts of all HB errors, and **X** the state vector containing the real and imaginary parts of the state-variable (SV) harmonics. The HB equations of the circuit may be written in the form

$$\mathbf{E}(\mathbf{X_H}, \mathbf{X_B}, \omega_S, u) = \mathbf{0} \tag{5}$$

where the state vector has been subdivided into two subvectors $\mathbf{X_H}$, $\mathbf{X_B}$, containing components at the carrier harmonics (h = 0) and at the sidebands (h ≠ 0), respectively. If the circuit is autonomous, the carrier frequency ω_0 is one of the problem unknowns. In this case the imaginary part of one of the harmonic components at frequency ω_0 must be kept fixed [9], and is replaced by ω_0 in the vector $\mathbf{X_H}$ [9]. On the contrary, if the circuit is forced by a sinusoidal source of frequency ω_0, the carrier is fixed, and $\mathbf{X_H}$ contains the real and imaginary parts of all the carrier harmonics. The effects of all driving sources (DC bias and microwave if existing) are included in the nonlinear operator **E**(•). In this way the formulation of the system (5) is equally valid for spurious analysis in forced circuits and in oscillators. On the other hand, the circuit is always autonomous with respect to the spurious oscillation. Thus ω_S is always a problem unknown, and the imaginary part of one of the SV harmonics at frequency ω_S is kept fixed (usually to zero), and does not appear in the vector $\mathbf{X_B}$ [9]. This harmonic will be referred to as the "reference harmonic" in the following. The reference harmonic is selected to belong to a state variable directly affecting the spurious output power, such as the drain voltage of the output stage for a FET oscillator or amplifier, and the like. Its real part will be denoted by X_R, while its imaginary part is zero, as already mentioned.

In the state space, a quasi-periodic solution path bifurcates from the periodic solution path at a Hopf bifurcation [1], [5]. When the circuit state approaches the Hopf bifurcation on the quasi-periodic path, then simultaneously $u \rightarrow u_H$, $\omega_S \rightarrow \omega_H$, $X_R \rightarrow 0$. It is thus obvious that an approximate evaluation of u_H, ω_H, or equivalently an approximate solution of (4), can be obtained by searching for a quasi-periodic regime having near-zero X_R. The normal procedure followed in the construction of the solution path is to assign the free parameter u, and to solve then (5) for $\mathbf{X_H}$, $\mathbf{X_B}$, ω_S. In order to approximately locate the Hopf bifurcation according to the preceding discussion, we interchange the roles of X_R and u, and treat the former as a known quantity, and the latter as a problem unknown. Thus X_R is fixed to a suitably small value, and (5) is solved by a Newton iteration for $\mathbf{X_H}$, $\mathbf{X_B}'$, ω_S, u, where $\mathbf{X_B}'$ is the vector obtained from $\mathbf{X_B}$ after suppressing X_R. Note that X_R cannot be set to zero, since the Jacobian of (5) would then be singular because of (4). Thus a suitable tradeoff must be sought between accuracy and convergence. If X_R is a drain voltage, it has been found that letting $X_R \approx 10^{-4}$ V still ensures excellent convergence, and allows u_H, ω_H to be evaluated with a relative accuracy typically better than 10^{-3}. The approximate location of a Hopf bifurcation by this technique takes a CPU time of the order of a few seconds on an HP 9000/750.

AUTOMATIC CONSTRUCTION OF HOPF BIFURCATIONS LOCI

The approximate technique discussed in the previous section can only perform a *local* search for the Hopf bifurcation, in the sense that the Newton iteration will only converge if the starting point is close enough to the bifurcation. As such, this method is not a substitute for *global* search algorithms of the kind discussed in [6], which can locate all the Hopf bifurcations of a parametrized circuit even if no starting-point information is available. However, the local algorithm is ideal for efficiently generating by continuation [10] Hopf bifurcations loci in a multidimensional parameter space, starting from any of the bifurcations located by the global algorithm. This technique is discussed in detail below. A similar method is obviously usable in the simpler case of (primary) Hopf bifurcations of DC states.

Although in principle the number of free parameters is arbitrary, we shall only consider two-dimensional parameter spaces for ease of graphical display of the loci. Let the circuit be parametrized by two independent parameters u_1, u_2. According to the discussion of the previous section, X_R is always fixed to some suitably small value, so that $\omega_S \approx \omega_H$, and the equation of the locus can be written in the form

$$\mathbf{E}(\mathbf{X_H}, \mathbf{X_B}', \omega_H, u_1, u_2) = \mathbf{0} \tag{6}$$

where the indication of X_R has been suppressed for simplicity. At each point of the locus, one of the two parameters actually plays the role of the independent variable, and is suitably stepped in order to generate the next point. (6) is then solved either for the set of unknowns $\mathbf{Y_1} = [\mathbf{X_H}, \mathbf{X_B}', \omega_S, u_1]$ (if u_2 acts as the free parameter), or for $\mathbf{Y_2} = [\mathbf{X_H}, \mathbf{X_B}', \omega_S, u_2]$ (if the reverse is true). The decision as to which parameter should be stepped is taken on the basis of the derivative Du_i/Du_j, which can be evaluated from (6) as

$$\frac{Du_i}{Du_j} = -\,\mathbf{R}\left[\mathbf{J}(\mathbf{Y_i})\right]^{-1} \left(\frac{\partial \mathbf{E}}{\partial u_j}\right)\Bigg|_{\mathbf{Y_i}\,=\,\text{const.}} \tag{7}$$

where the symbol D indicates that the derivative is taken along the locus, and **R** is the row matrix [0 0 0 ... 1]. The Jacobian matrix $\mathbf{J}(\mathbf{Y_i})$ is defined by

$$\mathbf{J}(\mathbf{Y_i}) = \left(\frac{\partial \mathbf{E}}{\partial \mathbf{Y_i}}\right)\Bigg|_{u_j=\text{const.}} \tag{8}$$

In practice, u_i is chosen as the independent parameter if the magnitude of (7) does not exceed a specified threshold. Otherwise the roles of the two parameters are interchanged. In this way the algorithm can automatically overcome any turning point that may be encountered on the locus. Once the independent parameter has been selected (say, u_j), the next point of the locus can be efficiently found by a simple

predictor-corrector scheme. In the predictor step, the increment of $\mathbf{Y}_i$ corresponding to an increment δu_j of the free parameter is estimated by application to (6) of the implicit function theorem:

$$\delta \mathbf{Y}_i \approx - \delta u_j \left[\mathbf{J}(\mathbf{Y}_i)\right]^{-1} \left(\frac{\partial \mathbf{E}}{\partial u_j}\right)\Bigg|_{\mathbf{Y}_i = \text{const.}} \tag{9}$$

The corrector step is just the solution of (6) by a Newton iteration starting from the point defined by (9). Note that the predictor step is virtually costless (except at those points where a parameter switching takes place), since the factorized Jacobian is automatically available after performing the corrector step for the previous point. The generation of a two-dimensional locus by this technique typically takes a few hundred seconds on an HP 9000/750.

APPLICATION TO BROADBAND VCO DESIGN

For illustrative purposes we consider the voltage-controlled oscillator whose topology is schematically illustrated in fig. 1. This VCO has to be designed for tunability over a 1 GHz band centered around 4.9 GHz as the varactor intrinsic bias voltage V is swept between zero and the breakdown voltage V_B = -25 V. Performance specifications include a minimum output power of 15 mW, a phase noise at 10 kHz offset from the carrier lower than -55 dBc/Hz, and a maximum deviation from linearity of ±80 MHz across the band. The purpose of the reactance-compensating network introduced on the gate (see fig. 1) is to provide the frequency dependence of the feedback reactance required for the linearization of the tuning characteristic. The resistor R is added for out-of-band stabilization. As in many broadband circuits, multiple resonances might occur owing to the relative complexity of the circuit topology, leading to the possible buildup of spurious oscillations. The detection and elimination of such spurious tones is an important aspect of the design problem.

As a first step, the VCO is optimized for the performance specifications and for synchronous stability by the method discussed in [4]. The optimization takes about 600 seconds on an HP 9000/750 and meets all the specifications. The resulting bifurcation diagram with the circuit parametrized by the varactor bias voltage is shown in fig. 2. Two independent periodic oscillation branches bounded by the primary Hopf bifurcations H_1, H_2, H_3, H_4, are observed. H_1PH_2 is the nominal solution path produced by the optimization, in the sense that the specifications are imposed on the circuit states belonging to this branch. H_3QH_4 is a spurious solution path autonomously generated by the circuit. For a given tuning voltage, the output powers at the two fundamentals, namely, p_1, p_2, are used as quantities synthetically representative of the system state on each periodic solution path. S_1, S_2 are (secondary) Hopf bifurcations of the periodic solution paths. In the state space S_1, S_2 are connected by a quasi-periodic branch which is not shown in fig. 2 for the sake of clarity [5]. Q, P in fig. 2 are defined as the points of the spurious and nominal periodic branches, respectively, associated with the same voltage values (namely, V_1, V_2) as the Hopf bifurcations S_1, S_2.

The resulting global stability pattern of the VCO may be described as follows [5]. The periodic branch H_1PS_1 is stable. The branch S_1H_2 of the nominal solution path is asynchronously unstable because of two complex conjugate natural frequencies with positive real parts. The stability pattern on the spurious solution branch is similar in the forward voltage sense. The periodic branch H_4QS_2 is stable, and becomes asynchronously unstable between S_2 and H_3. The turning point T_1 introduces a positive real natural frequency, so that the branch T_1H_3 of the spurious solution path is synchronously unstable as well. All the remaining periodic states are synchronously stable. The quasi-periodic solution path bifurcating from S_1 and S_2 is completely unstable, so that its interest is marginal for the sake of the present discussion. Thus the VCO exhibits jumps (from one periodic branch to the other) when it is tuned past S_1 on the nominal branch or past S_2 on the spurious one. This originates a hysteresis cycle PS_1QS_2. Note that these jumps are profoundly different in nature from those discussed by Kurokawa [11], which are simply due to the occurrence of synchronous instabilities on the nominal periodic solution path. What is more important, the VCO is bistable in the voltage range $V_1 \le V \le V_2$ (i.e., the shaded region in fig. 2). This means that if the drain bias is turned on with the varactor biased within this range, either the nominal or the spurious oscillation will build up with equal probability, depending on the noise waveforms that actually excite the oscillation startup.

The VCO behavior as described above is obviously not acceptable, and a further design step must be carried out in order to suppress any kind of asynchronous instability. For this purpose, a number of two-dimensional Hopf bifurcations loci were built in order to visualize the dependence of the spurious generation mechanism on selected circuit parameters. The most interesting result is given in fig. 3. In this figure one of the parameters is the varactor bias voltage, which implicitly carries the information on the VCO tuning range, and the other one is the resistance R shown in fig. 1. The figure simultaneously shows the loci of the four primary Hopf bifurcations H_1, H_2, H_3, H_4, and of the two secondary Hopf bifurcations S_1, S_2. The generation of fig. 3 takes about 1400 seconds on an HP 9000/750. Fig. 3 provides some interesting design information. Both the secondary Hopf bifurcations and the spurious periodic branch are seen to disappear at all when R exceeds a threshold value $R_T \approx 134\ \Omega$. The value $R_0 = 50\ \Omega$ selected by the initial optimization falls well within the region where spurious generation takes place. Of course, simply setting R to a value larger than R_T would considerably degrade the remaining aspects of the circuit performance. We thus carry out a second design step consisting of a new optimization starting from the final point of the previous one, but with the added constraint $R > R_T$. The final optimization takes about 40 seconds on an HP 9000/750 and once again meets all the specifications. The resulting bifurcation diagram given in fig. 4 describes a very well-behaved tunable oscillator, completely free of instability phenomena of any kind.

CONCLUSION

The paper has shown that existing HB-based CAD methods for the numerical design of broadband nonlinear subsystems, can be extended to include the requirement that the circuit be spurious-free. The proposed approach is an interactive technique based on the alternate use of state-of-the-art optimization and numerically generated Hopf bifurcations loci. The latter are shown to represent a very powerful engineering tool, providing a synthetic overview of the influence of selected parameters on the entire circuit bifurcation pattern. This allows the spurious generation process to be understood by the circuit designer, and to be prevented by intelligent interventions that would be fatally beyond the reach of any conventional optimization method. For typical microwave subsystems the generation of two-parameter Hopf bifurcations loci is fast enough to be compatible with the requirements of workstation-based CAD.

ACKNOWLEDGMENTS

This work was partly sponsored by the Italian Space Agency (ASI) and by the Istituto Superiore delle Poste e delle Telecomunicazioni (ISPT).

REFERENCES

[1] J. Guckenheimer and P. Holmes, *Nonlinear Oscillations, Dynamical Systems, and Bifurcations of Vector Fields*. New York: Springer-Verlag, 1983.

[2] V. Rizzoli and A. Neri, "State of the art and present trends in nonlinear microwave CAD techniques", *IEEE Trans. Microwave Theory Tech.*, Vol. 36, Feb. 1988, pp. 343-365.

[3] V. Rizzoli, A. Costanzo, and A. Neri, "Automatic generation of the solution path of a parametrized nonlinear circuit in the presence of turning points", *Microwave Opt. Tech. Letters*, Vol. 7, Apr. 20, 1994, pp. 270-274.

[4] V. Rizzoli, A. Costanzo, F. Mastri and C. Cecchetti, "Harmonic-balance optimization of microwave oscillators for electrical performance, steady-state stability, and near-carrier phase noise", *1994 IEEE MTT-S Int. Microwave Symp. Digest* (San Diego), May 1994, pp. 1401-1404.

[5] V. Rizzoli, A. Neri, and G. Righi, "Analysis of spurious tones in microwave oscillators via the Hopf bifurcation concept", *Proc. 24th European Microwave Conference* (Cannes), Sep. 1994, pp. 836-841.

[6] V. Rizzoli and A. Neri, "Automatic detection of Hopf bifurcations on the solution path of a parametrized nonlinear circuit", *IEEE Microwave Guided Waves Letters*, Vol. 3, Jul. 1993, pp. 219-221.

[7] R. Queré *et al.*, "Large signal design of broadband monolithic microwave frequency dividers and phase-locked oscillators", *IEEE Trans. Microwave Theory Tech.*, Vol. 41, Nov. 1993, pp. 1928-1938.

[8] V. Rizzoli *et al.*: "State-of-the-art harmonic-balance simulation of forced nonlinear microwave circuits by the piecewise technique", *IEEE Trans. Microwave Theory Tech.*, Vol. 40, Jan. 1992, pp. 12-28.

[9] V. Rizzoli and A. Neri, "Harmonic-balance analysis of multitone autonomous nonlinear microwave circuits", *1991 IEEE MTT-S Int. Microwave Symp. Digest* (Boston), Jun. 1991, pp. 107-110.

[10] H. Wacker, *Continuation Methods*. New York: Academic Press, 1978.

[11] K. Kurokawa, "Injection locking of microwave solid-state oscillators", *Proc. IEEE*, Vol. 61, Oct. 1973, pp. 1386-1410.

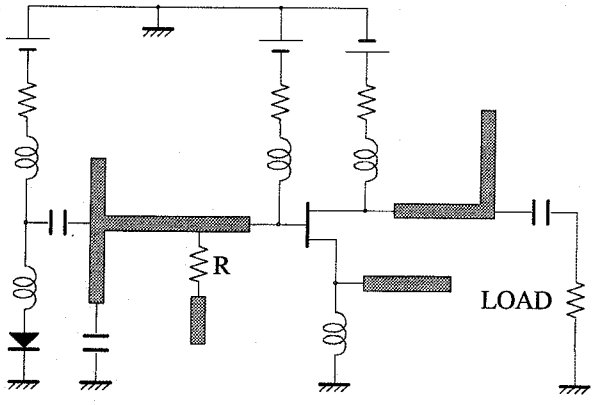

Fig. 1 - Schematic topology of a broadband VCO

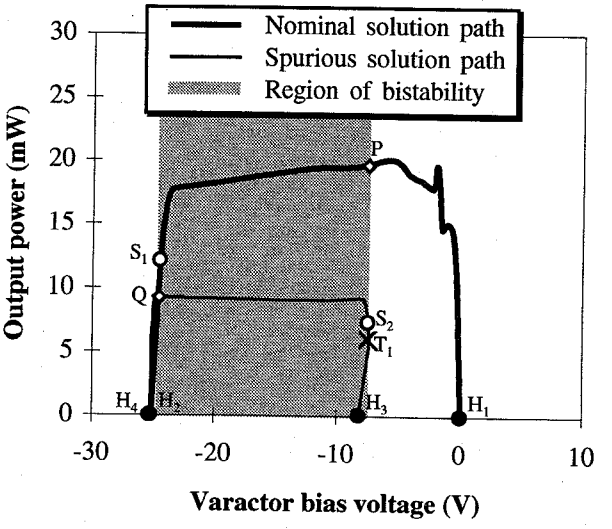

Fig. 2 - Bifurcation diagram for the VCO in fig. 1

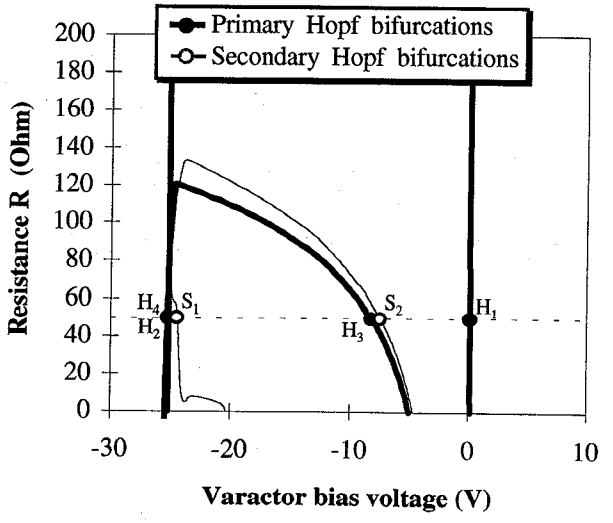

Fig. 3 - Loci of primary and secondary bifurcations for the VCO in fig. 1

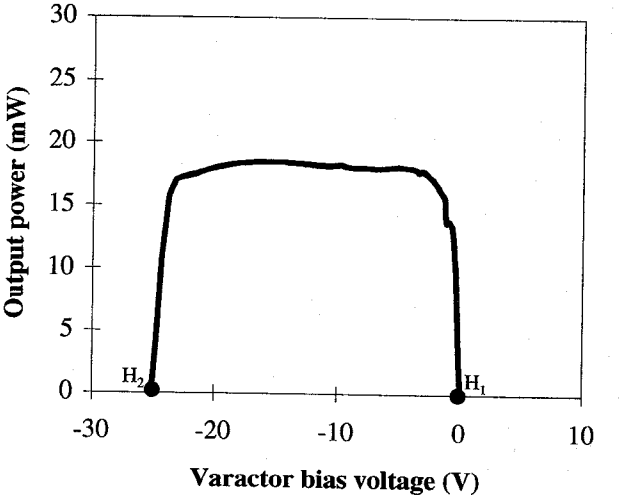

Fig. 4 - Bifurcation diagram for the optimized VCO